ÉCOLE POLYTECHNIQUE
FÉDÉRALE DE LAUSANNE

SEMESTER PROJECT

Bio-Inspired Foot Design for a Salamander Robot

Student:

Patrick SCHWIZER

Advisor:

Dr. Kostas KARAKASILIOTIS

Professor:

Prof. Auke Jan IJSPEERT

January 10, 2014

Contents

List of Figures

List of Tables

1 Introduction

The study of animal locomotion is nowadays closely related to robotics. Bio-inspired robots are therefore used to study and reproduce animal locomotion patterns and neural networks. But one aspect has not been studied yet in depth: the role of fingers and compliance at the foot level.

Nowadays, most of the existing robots do not use fingers, but they could actually improve different characteristics of the whole system because they equip the robot with additional adaptability and compliance at the foot level. Some of these improvements might be: better traction, terrain adaptation, increased speed, locomotion efficiency, additional damping and swimming efficiency.

In order to study the role of compliance and fingers at the foot level, this project aims at designing a bio-inspired foot for a salamander robot. In a first step, the anatomy of a salamander is studied and on the basis of this analysis, a foot is designed. In a first approach, in the scope of this project, only passive elements are used therefore.

To actually test and verify the final design of the foot with fingers, prototypes have to be built and tested with the existing salamander robot.

2 Problem Definition

The Pleurobot, see figure 1 is a salamander-like quadruped robot. Its new biomimic approach which bases on 3-dimensional X-ray scans allows to reproduce the movements of the animal in three dimensions with a reasonable accuracy. For further details, see [3]. So far, the Pleurobot is mainly tested with the basic ball feet, see also figures 5 and 6.

Figure 1: Pleurobot with ball feet

2.1 Problem Scope

To study the influence of compliant feet and the role of fingers in salamander locomotion, the Pleurobot needs to be equipped with new feet.

This project therefore aims at designing more sophisticated, bio-inspired hind limbs for Pleurobot. The forelimbs are less complex and can be considered as a ball foot with fingers and are not treated in this report.

2.2 Technical Review

In a first step, the anatomical background of salamander feet is studied, see section 2.2.1. Furthermore, the already existing technical solutions of salamander feet are analysed in sections 2.2.2 and 2.2.3. On the basis of these analyses, the design requirements can be defined in section 2.3.

2.2.1 Anatomical Background

The foot of the salamander can be divided into 4 parts, see also figure 2:

Crus is the part between the knee and the ankle joint. The design of the compliant foot for this projects starts at the crus. The crus of the robot is represented as a metal bar, to which the foot is attached.

Tarsus & Metatarsus build together the foot palm.

Phalanges are the fingers and are extensions of the metatarsals.

The relative angles between the different foot parts during the step cycle are shown in figure 3. Especially figures **D**, **E** and **F** are of interest for the design of the new foot.

By analysing the video of Reza, see figure 4, one can see, that the tarsus actually never touches the ground through the whole step cycle. It maintains at least an angle of about 20° with respect to the ground. Furthermore, the direction of the foot respectively the fingers stays the same for the whole step cycle. To allow this behaviour, first, the ankle is twisted, see figure 3 **E**. Then, this rotation is blocked and the twisting between the metatarsals and the phalanges start, see figure 3 **F**. By having constant a contact between the fingers and the ground, static friction is guaranteed. The salamanders have a better traction and a higher locomotion efficiency like that.

The angular kinematics and the study of the video with the fitted bones establish the basis for the design requirements and the new foot design.

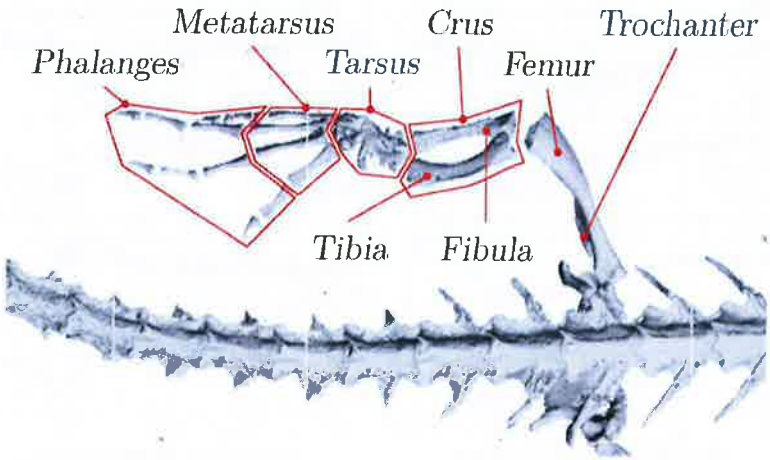

Figure 2: Anatomy of a salamander foot

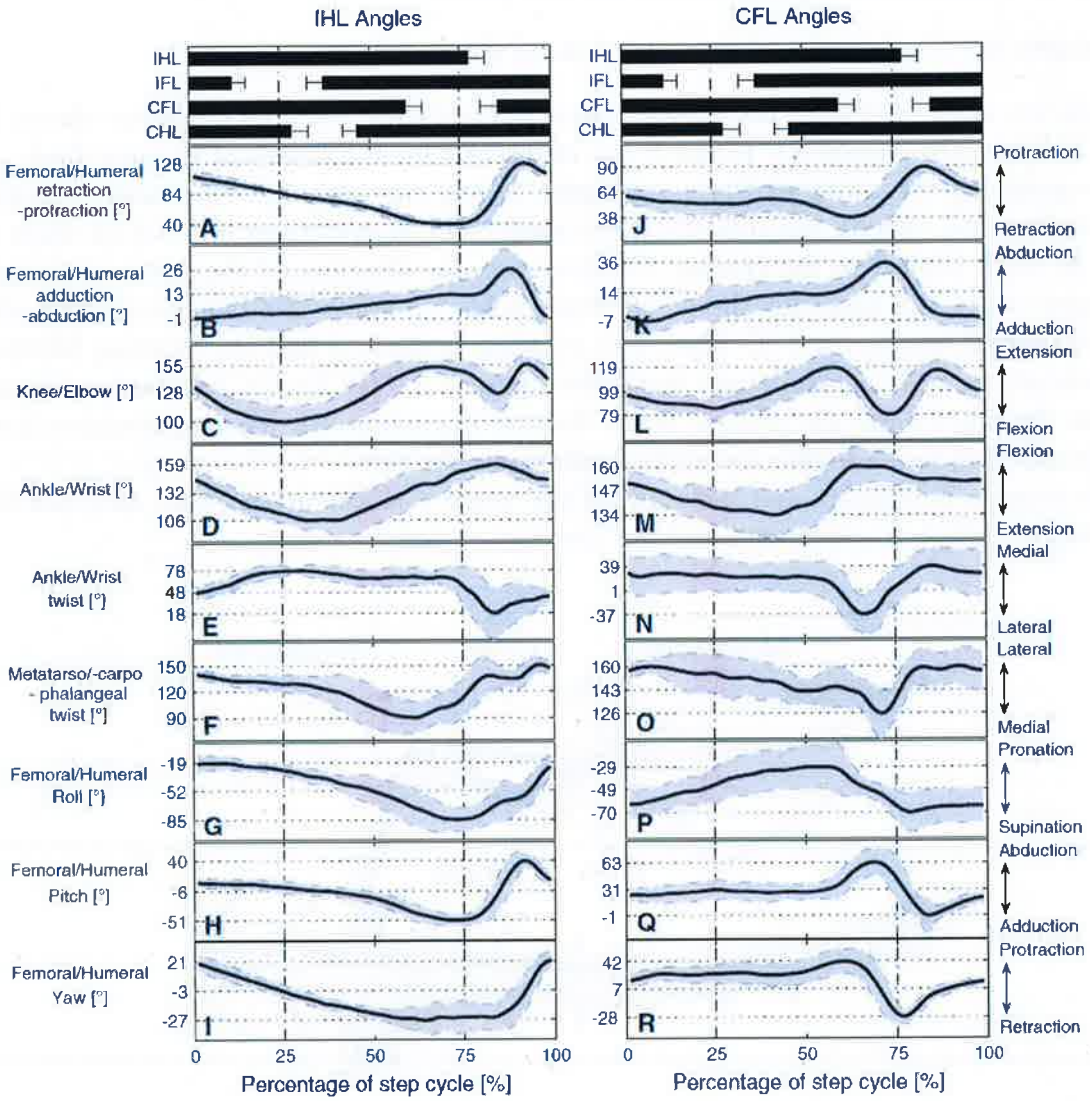

Figure 3: Angular kinematics of the ipsilateral hindlimb (IHL) and the contralateral forelimb (CFL) [1]

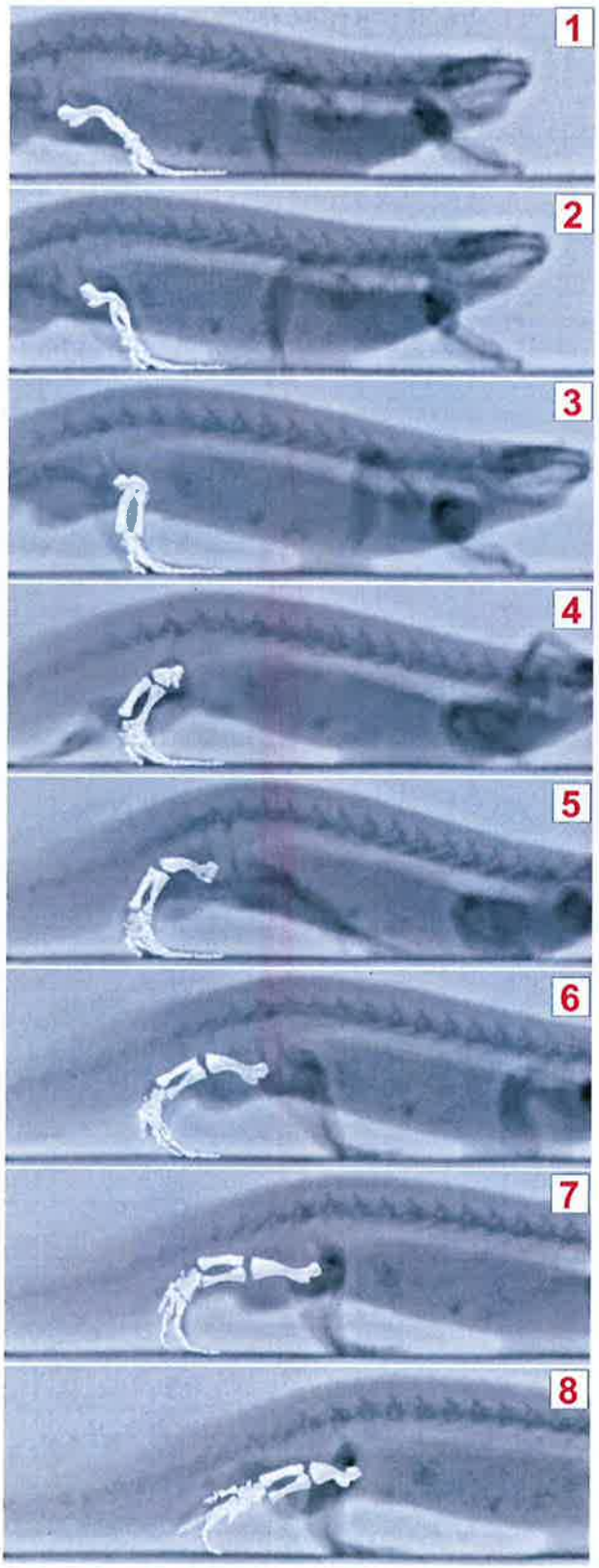

Figure 4: Sequences of 3-dimensional X-ray video with bone fitting [2]

2.2.2 Ball Foot

The ball foot is the first and the simplest representation of the salamander foot for Pleurobot. The surface of the sphere represents the end of the metatarsals. It is therefore like a foot without the fingers.

Its core consists of 3-D printed ABS polymer and is directly attached to the metal bar respectively the crus. Around this core, silicone rubber is moulded in order to improve traction and to add some compliance.

The ball foot works very well and it is very stable due to its low number of parts and because there are no moveable parts. But evidently, this design does not allow the testing of fingers.

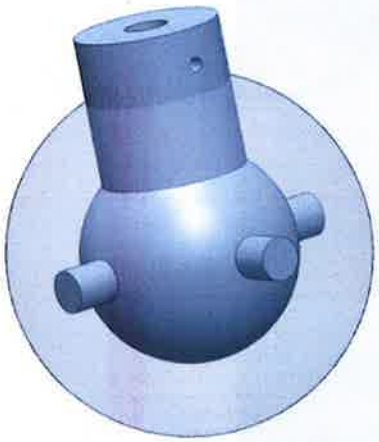

Figure 5: Ball foot [2]

Figure 6: Pleurobot with ball foot [2]

2.2.3 Foot with Compliant Fingers and Ankle Joint

A more sophisticated approach is the foot with an ankle joint and compliant fingers, see figure 7. The ankle joint consists of a ball joint, which allows the rotation in all three directions. To regulate the stiffnesses in all directions of this joint, springs are attached between the metal bar and the tarsus. The fingers consist of nitinol wires, 10 wires of $0.5\,mm$ for each finger. At the end of the fingers, hot glue drops increase the traction and hold the nitinol assemblies in position. Furthermore between the fingers and the rigid tarsus, there are pre-tensioned hinge joints.

Nitinol is a nickel-titanium allay and it is a superelastic material that supports large deformations without plasticity. In section 3, nitinol will also be used for the new designs.

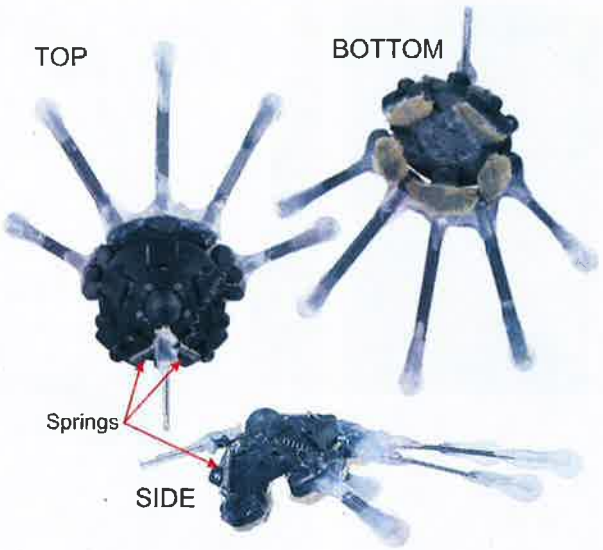

Figure 7: Foot with compliant fingers and ankle joint [2]

Problems with Compliant Finger Foot

In the video analysis, see figure 8, one can see that the direction of the foot does not stay constant during the step cycle. By having dynamic and not static friction, the efficiency is reduced.

Furthermore, video analysis revealed, that the tarsus is in contact with the ground during the whole stance phase.

These two properties of this foot version are in conflict with the observation of the real foot, presented in section 2.2.1. The problem bases on the different stiffnesses of the ball joint: The torsional stiffness is too high, which results in the rotation of the foot. The deflection stiffness in the lateral direction is too low and therefore the tarsus touches the ground.

As the ball joints allows a rotation in all three directions, it is almost impossible to have different stiffnesses for the different degrees of freedom with this solution.

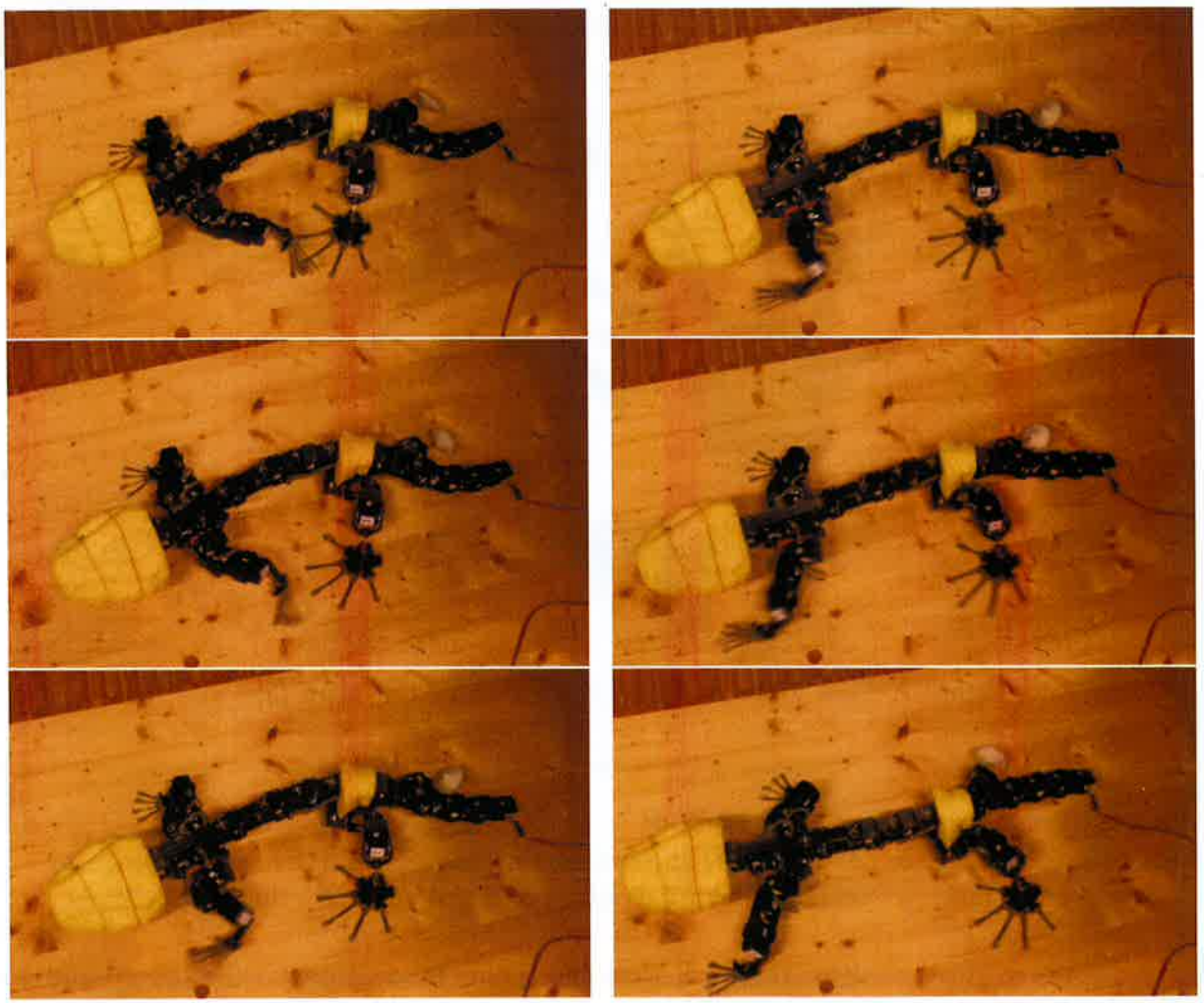

Figure 8: Video analysis of previous tests

2.3 Design Requirements

The design requirement can be divided into geometrical requirements mainly based on the anatomy, see section 2.3.1 and construction-related requirements, see section 2.3.2

2.3.1 Geometrical Requirements

The geometrical requirements define the range of the degrees of freedom, see table 1 and the dimensions of the parts, see table 4. Only the ranges of the ankle joint are defined, as this joint is the crucial one and the other joints, i.e. between metatarsals and phalanges follow the movement and do not have well-defined end blocks.

Furthermore, as presented in 2.2.1, the tarsus should not touch the ground and keep a minimal angle of 20° to the ground.

Another requirement concerns the attachment of the foot to the robot. It has to be realised by the metal bar, see figure 9. The bar has a diameter of $5\,mm$.

Table 1: Geometrical requirements for the ankle joint

Direction	Value
Twist	18° - 78°
Lateral bending	106° - 159°
Longitudinal bending	no data available. DOF should avoid the longitudinal rotation of the foot with respect to the ground.

Table 2: Dimension of the animal and the robot parts

Dimension	Animal value $[mm]$	Robot value $[mm]$
Crus	6.7	58.49
Tarsal length	4.8	41.9
Metatarsals & Phalanges (max. value)	10	87.3

2.3.2 Construction Related Requirements

The construction related requirements assure a proper functioning in diverse environments. They cannot be checked objectively like the geometrical requirements, but they serve as design guidelines.

Appearance The appearance of the foot should be as close as possible to the appearance of the natural foot.

Water resistance In order to test the swimming efficiency of the robot with the new feet, they have to be water resistant.

Robustness So that the robot can be used in as many conditions as possible, the functioning of the foot has to be as robust as possible. Therefore it is appreciated to have an as simple and robust mechanism as possible in order to prevent failures.

Figure 9: Connection bar

Mud & grass tolerance In order to use the robot in different environments, the robot must be mud and grass tolerant. That means that the joints must not be blocked by mud or grass so that the robot does not get stuck in these environments.

Materials All components of the foot have to be passive in order to keep the complexity as low as possible and to avoid control problems. The materials that can be used are described in table 3.

Table 3: Available materials

Material	Details
ABS	3-D printed
POM & Carbon plates	2-D contour milling
Silicone (see appendix ??)	moulded in ABS-mould
Nitinol-Wires	diameters: 1, 1.4 & 1.9 mm
Springs	various dimensions
Tubes & Axes	various dimensions
Screws & Nuts	various sizes

3 New Foot Designs

This section presents the two design which have been developed in this project. The version 1, the foot with defined joints, see section 3.1 is a further development of the foot presented in 2.2.3. In the second approach, see section 3.2 all rigid parts are replaced by compliant parts in order to have a completely compliant foot, from the crus to the toe-tips.

3.1 Foot with Defined Joints

As already mentioned, this version is a direct successor of the foot presented in section 2.2.3. Instead of having a ball joint with all three degrees of freedom in one joint, the two main rotations, i.e. the twisting and the bending in the lateral axes have been realised separately. Figure 10 shows the design when the foot is completely extended. The twist joint and the bending mechanism are presented in sections 3.1.1 and 3.1.2, respectively. The realised dimensions of the parts are presented in table **??**.

The assembly consists of three subassemblies: the metal bar on the very left, the mid-joint part with a box-shaped contour and the tarsus on the right with its fingers.

Table 4: Dimensions of model

Variable	Computed value $[mm]$	Realised value $[mm]$
Crus	58.49	70.36
Tarsal	41.9	42
Metatarsals & finger	87.3	70
Crus to fingertip	187.7	182.3

Figure 10: Isometric view of the extended foot

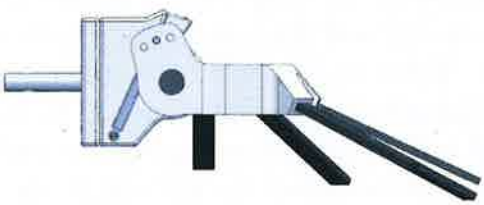

Figure 11: Side view of the extended foot

3.1.1 Twisting Joint

In order to avoid the rotation of the foot with respect to the ground, a twisting joint, see figures 12 and 13 is implemented between the metal bar and the mid-joint part. The longitudinal movement of the axis is blocked by a circular disk which is attached to the metal bar via a metal pin. To allow a proper rotation of the bar, gliding guides are force fitted into the mid-joint part, see L-shaped guides in figure 13. To align the foot boack to the initial position during the swing phase, a low-stiffness spring is attached between the mid-joint part and the axis, see figure 12. The maximum displacement angle is 60°, according to the geometrical requirements.

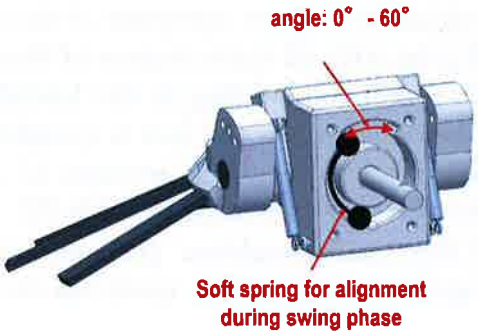

Figure 12: Twisting joint

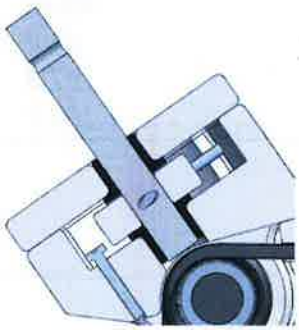

Figure 13: Cross-section through twisting joint

3.1.2 Bending Joint

Between the mid-joint part and the tarsus, a rotational joint is implemented that allows the foot to bend, see figure 16. In figure 16 **A**, one can see, that the joint actually consists of three moveable parts, attached to the same axis: The part connected to the crus bar (1), the holder of the pretension (2) and the tarsus (3). Figure 14 shows the stiffness of this joint over its whole range. When the angle between the tarsus and the metal is lower than 0°, as in state **A**, the stiffness is low and only applied by the tension spring, seen in figure 11. The stiffer torsional springs are not yet applied to part (1) as they are blocked by part (2), of which the range is restricted by the screw, see red circle in figure. By increasing the angle from **B** to **C**, the stiffness suddenly increases as the torsional springs are applying their moment to both parts (1) and (2). The final state is represented in figure **D**.

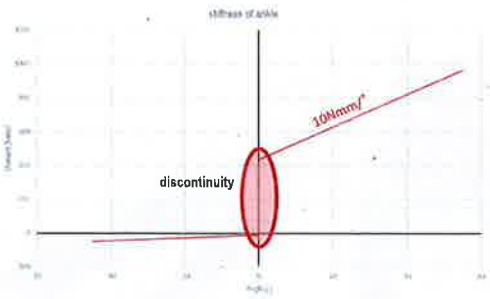

Figure 14: Stiffness graph of ankle bending

Calculation of Joint Stiffness

The stiffness needed in this joint, was evaluated by setting the required resulting moment at two different states, see table 5 and figure 15. The first state is when the foot touches the ground and the second one when the knee is over the point of contact of the foot with the ground. The vertical ground reaction force at footfall is about $10\,N$ and reaches the maximum of $40\,N$, when the knee is over the point of contact. The torsional springs are pre-tensioned with an angle of $45\,degrees$. The equation assumes a quasi-static state and sets the moment of the torsional springs equal to the moment applied by the ground reaction force. With this equation and the two states, one can solve the equation for the stiffness. For the first state, the optimal stiffness is: $8.8\,Nmm/°$, the optimal stiffness for the second state $11.9\,Nmm/°$. Therefore, in a first approach, the stiffness of the torsional springs is set to $10\,Nmm/°$.

$$(angle_{crus} - angle_{tarsus} + angle_{pretension}) * stiffness = length_{tarsus} * cos(angle_{tarsus}) * GRF_z$$

Table 5: States for stiffness calculation

	$angle_{crus}$ [°]	$angle_{tarsus}$ [°]	GRF_z [N]
state 1	20	20	10
state 2	100	45	40

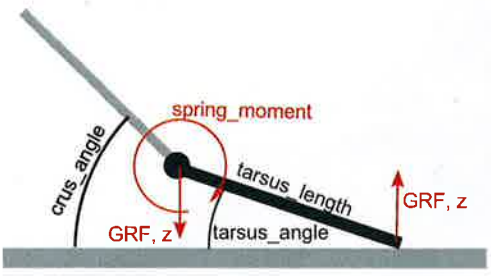

Figure 15: Schema of forces and moments acting on the tarsus

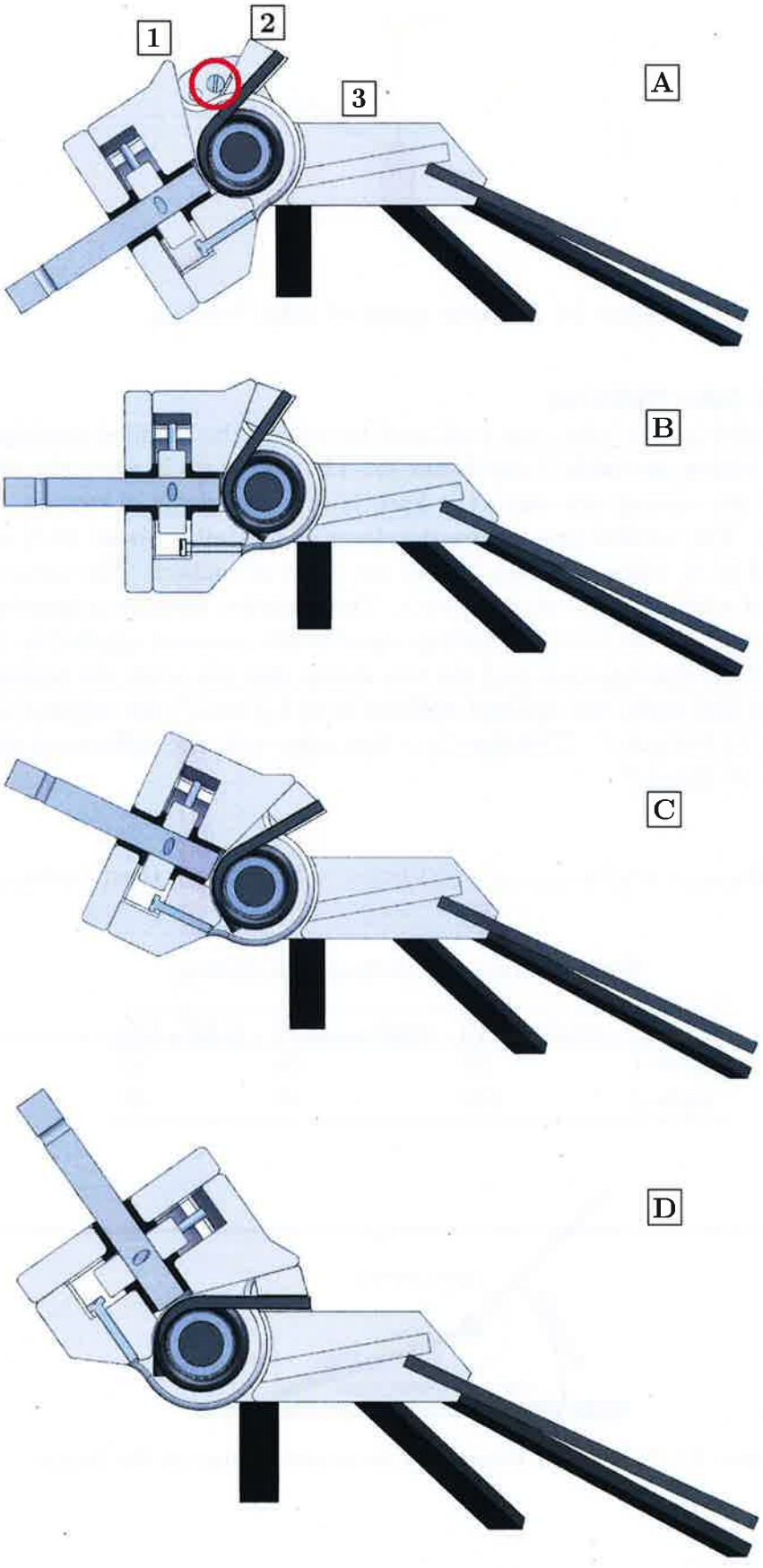

Figure 16: Sequence of bending mechanism

3.2 Compliant Foot

The second version is a completely compliant foot, see figure 17. The outer contour imitates the foot of a salamander and consists of silicone. To make the whole structure stiffer in order to be able to bear the robot structure, which weights about $8\,kg$, nitinol wires are implemented. The wires are attached to the rigid connection part, see figure 18. On the opposite side of this connection part, the metal bar is attached. Several holes in this connection part allow a good connection between to the silicone.

The caps at the ends of the nitinol wires prohibit the destruction of the silicone material by the sharp edges of the wires.

Table 6: Dimensions of model

Part	Computed value $[mm]$	Realised value $[mm]$
Crus	58.49	60
Tarsal & metatarsal		67
Finger		60
Tarsal	41.9	
Metatarsal & finger	87.3	
Crus to fingertip	187.7	187

Figure 17: Completely compliant foot

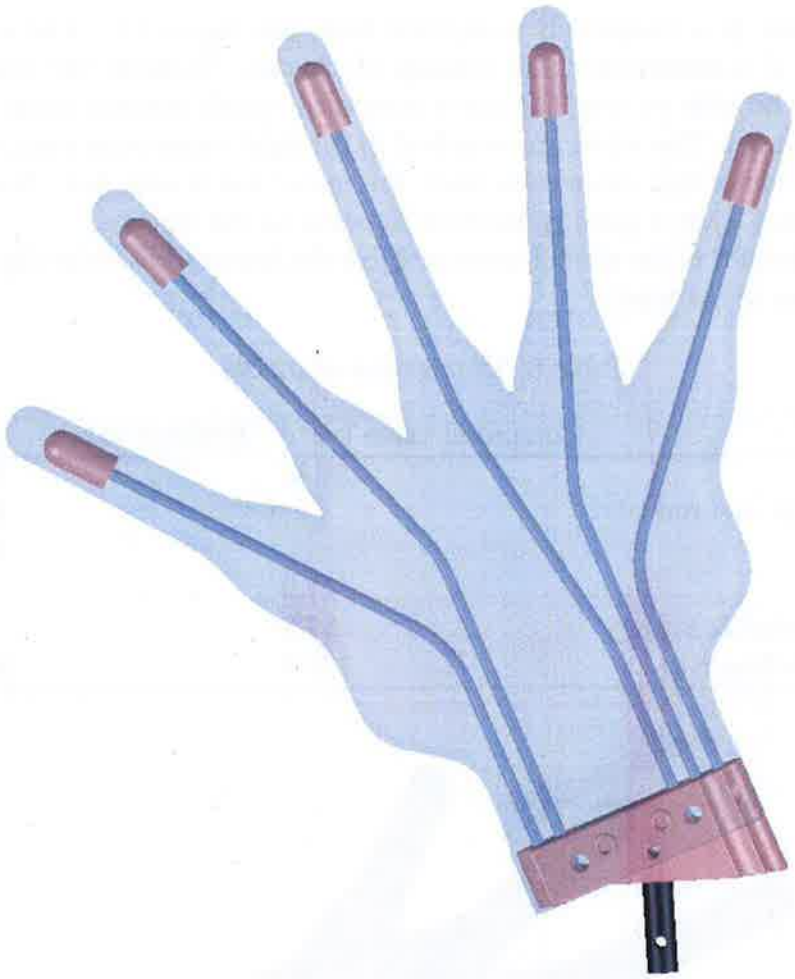

Figure 18: Top view of compliant foot with transparent silicone

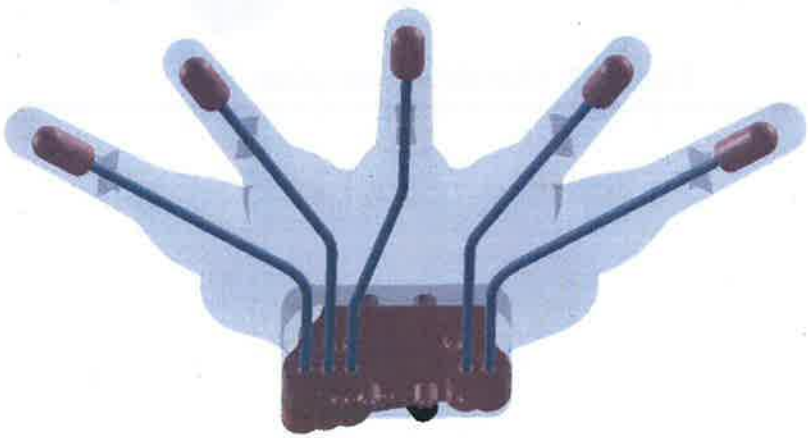

Figure 19: Front view of compliant foot with transparent silicone

4 Evaluation of Designs

4.1 Overview

This section describes the manufacturing of the prototypes in the following text part 4.2 and the testing of these prototypes in section 4.3. Of each version, one prototype was built and tested, for both versions the left foot, as the kinematics was only ready for this side.

4.2 Prototypes

4.2.1 Prototype 1

Almost all parts of this version were 3-D printed with ABS. Only the circular disk that is attached to the metal bar and the cover plate are milled out of a POM-plate. The fingers are the same as for the version in figure 7.

4.2.2 Prototype 2

The first step in the production of version two was to bend the nitinol wires to the desired shape. They were heated over a candle and bent by hand to the right form. The 5 caps at each finger and the connection part are made out of 3-D printed ABS. All of these parts together build the skeleton of the hand. Then, silicone is moulded around. Therefore, an ABS-mould was 3-D printed, see figures 20 and 21. The skeleton is then positioned and fixed inside the form via 4 metal pins. After the closure of the two parts, they are pressed against each other. Then, the 2-component silicone, see appendix **??** is mixed and poured into the form. In order to avoid that the silicone gets too viscous to pour before the whole form is filled, it is recommended to prepare about 3 times a mixture with 2 spoons of each component. The hardening time is about 30 minutes.

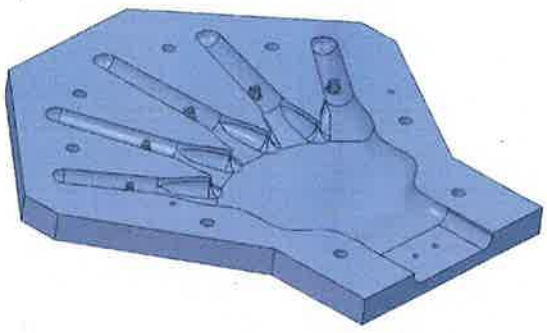

Figure 20: Bottom part of the mould

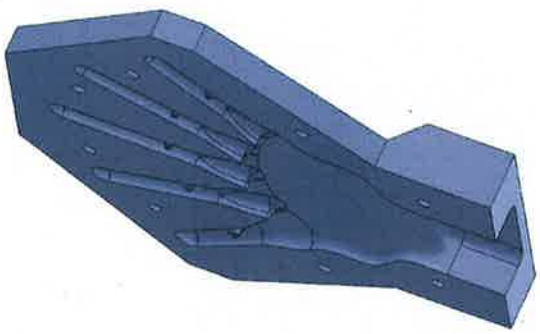

Figure 21: Top part of the mould

4.3 Testing and Results

To test the prototypes, both versions were attached to the robot. Both tests were not successful. Figure 22 shows a sequence of the test-video of the compliant foot. Various problems were evaluated for both versions of the foot and the kinematics, which might not be good for a foot with fingers yet:

Kinematics problems:

- The foot is not aligned to the direction of locomotion at footfall, see figure 22.
- During the stance phase, the knee joint does not pass over the foot. It is more, that the foot is pulled around the knee joint.

Version 1

- The current kinematics of the robot does not have enough ground clearance of the foot during the swing phase. Therefore, the repositioning of the foot during the swing phase does not work properly and the foot is not extended at the footfall.
- The ABS-parts, especially part (2) in figure 16 bends under the load of the torsional springs and then the clearance between the parts disappears and the parts start to rub against each other during rotation.
- The foot does probably not have enough degrees of freedom, respectively the kinematics does not accord with only two degrees of freedom.

Version 2

- The twisting degree of freedom is probably too stiff.
- The silicone rips off at the fingertips, where the protection caps are. The thickness of the silicone is too small.
- The nitinol wires can turn inside the connection part.

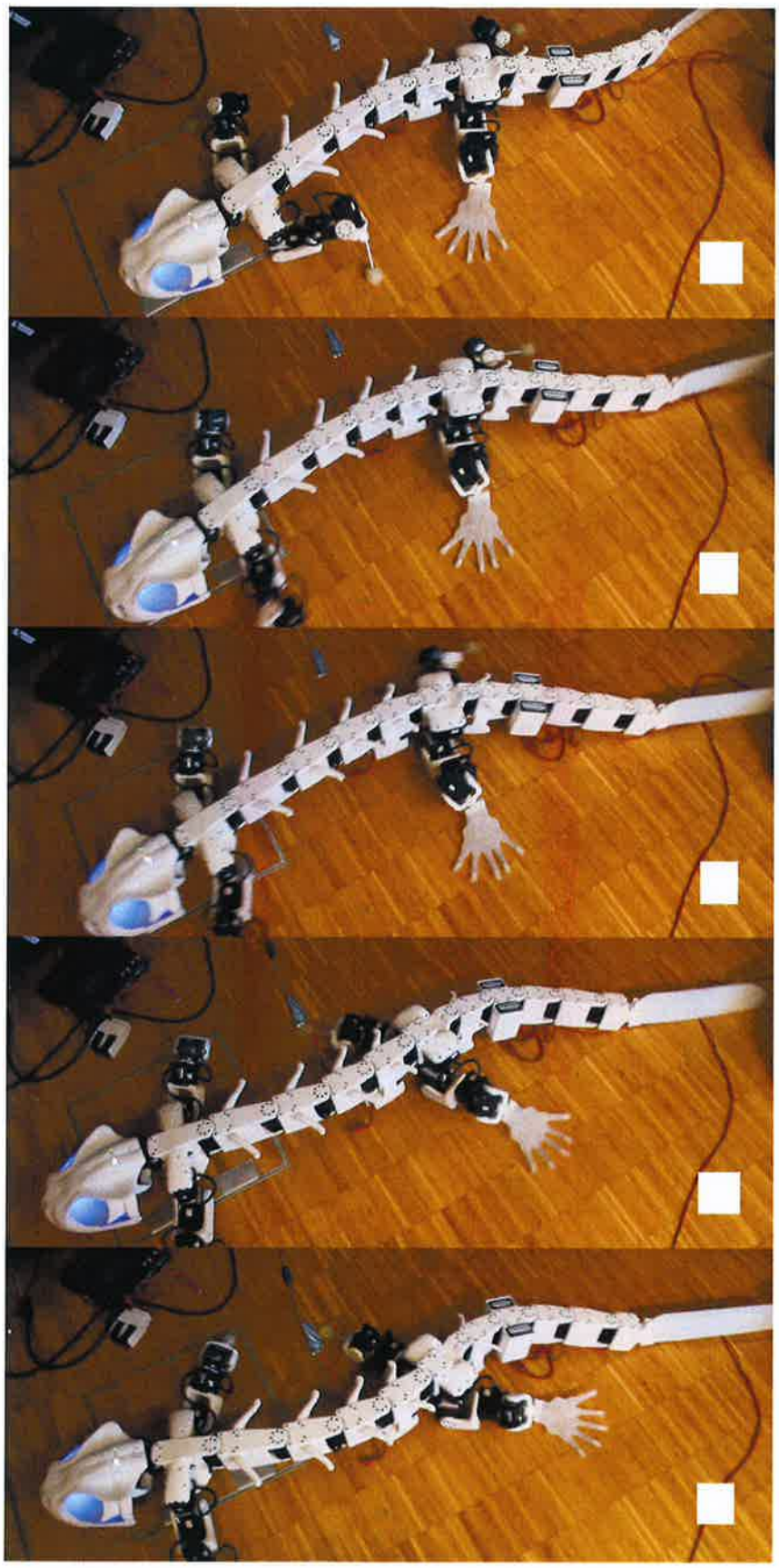

Figure 22: Sequences of testing video

4.4 Next Steps

As the optimal solution to test the role of fingers and compliance is the completely compliant foot, version 2, only this version should be followed. To improve the properties of this foot, various approaches can be considered:

- try different nitinol diameters for fingers or combine different diameters in the same version
- make several rigid elements and connect them via flexible elements -> possibility to regulate stiffnesses for different areas
- add twisting joint like for the version 1 in order to eliminate rotational slipping of the foot
- make all wires exactly straight to avoid the twisting of the wires inside the connection part
- for bent nitinol wires, block twisting of wires completely (form-locking)
- use active elements, for example nitinol wires can be used as "muscles"
- ball-foot with linear actor -> extend at the end of the stance phase to simulate the longer ground contact added by the fingers

Furthermore, the kinematics will need to be optimised for the foot with fingers.

5 Conclusion

By analysing the anatomy of the salamander and the older foot versions, two new foot designs were developed. The complexity of the kinematics and the interaction of all elements was underestimated. At a first sight, this development seemed straightforward and no tests were carried out with the first version until the second prototype was built. The assumption, that both versions will work was refuted by the tests and it was too late to react. Therefore, for future projects about this topic, it is very important to start experimental analysis at an earlier stage of the project. It can be seen that analytically, the behaviour of the compliant salamander foot is almost impossible to capture and to reproduce technically. Furthermore, the importance of the robot kinematics was not considered. Future projects therefore have to develop a compliant foot together and with respect to the kinematics of the robot.

The goal of this project was to determine the role of the fingers and compliance at foot level. With none of the prototypes, this properties can be analysed at the moment.

References

[1] Konstantinos Karakasiliotis, Nadja Schilling, Jean-Marie Cabelguen, and Auke Jan Ijspeert. Where are we in understanding salamander locomotion: biological and robotic perspectives on kinematics. *Biological Cybernetics*, 107(5):529–544, Oct 2013.

[2] Konstantinos Karakasiliotis. *Legged locomotion with spinal undulations*. PhD thesis, STI, Lausanne, 2013.

[3] Pleurobot. Web, 11 2013. http://biorob.epfl.ch/pleurobot.

Appendix A Datasheet of Silicone

NEUKASIL SN 2850 (SCS-RTV-Silikon 2850)

Siliconkautschuk
additionsvernetzend

Haupteigenschaften

- gute Ein- und Weiterreißfestigkeit
- sehr gut fließend
- thixotropierbar
- Mischungsverhältnis A : B = 1 : 1
- schnelle Durchhärtung

Anwendungen

- allgemeiner Formenbau
- Körperabformung
- Herstellung von Formen für Schokolade, Marzipan u.ä..

Eigenschaften im unvernetzten Zustand (ca. Werte)

				NEUKASIL SN 2850 Komp.A	NEUKASIL SN 2850 Komp.B
Farbe				transluzent	transluzent
Dichte 20 °C	g/cm³			1,04	1,05
Viskosität 20°C	mPas			2.600	3.000

Eigenschaften der Mischung (ca. Werte)

Mischungsverhältnis	Gew. Teile			100	100
Mischviskosität 20°C	mPas				2.800
Verarbeitungszeit	(1000g) Minuten				5
Aushärtungszeit	Minuten				30
Härte (24h)	Shore A	DIN 53505			23
Härte (7d)	Shore A	DIN 53505			23
Gebrauchstemperatur kurzfristig	°C				200
Reißfestigkeit	N/mm²	DIN 53504 S2			2,5
Reißdehnung	%	DIN 53504 S2			600
Weiterreißfestigkeit	N/mm	ASTM 624 B			11,0
Lineare Maßänderung	%				< 0,2

Verarbeitungsbedingungen

Wichtiger Hinweis: Der Platinkatalysator befindet sich in der Komponente A.
Zur Herstellung eines verarbeitungsfähigen Ansatzes wird die notwendige Vernetzermenge zu dem Kautschuk gegeben und so lange eingerührt, bis eine homogene Verteilung erreicht ist.
Während des Mischens ist darauf zu achten, dass möglichst wenig Luft eingerührt wird.